Pergamon

SCIENCE DIRECT®

Tetrahedron 59 (2003) 175–185

TETRAHEDRON

Self-association and self-assembly of molecular clips in solution and in the solid state

Joost N. H. Reek,[a,†] Johannes A. A. W. Elemans,[a,*] René de Gelder,[b] Paul T. Beurskens,[b] Alan E. Rowan[a,*] and Roeland J. M. Nolte[a]

[a]*Department of Organic Chemistry, NSRIM, University of Nijmegen, Toernooiveld, 6525 ED Nijmegen, The Netherlands*
[b]*Crystallography Laboratory, Department of Inorganic Chemistry, NSRIM, University of Nijmegen, The Netherlands*

Received 15 July 2002; revised 21 October 2002; accepted 14 November 2002

Abstract—Clip molecules based on diphenylglycoluril form well-defined dimeric structures in chloroform solution and in the solid state. In solution the dimerization process is based on favourable π−π interactions and cavity filling effects. A combination of favourable π−π interactions and crystal packing forces determine the self-assembly of clips in the solid state. The geometry that the clip molecules adopt in solution and in a series of X-ray crystal structures is compared with favourable geometries predicted by molecular modelling calculations.

1. Introduction

The self-assembly of relatively simple building blocks is a topic of great interest in modern supramolecular chemistry, since many biological systems are constructed by hierarchical self-assembly processes.[1,2] These processes can lead to complex multicomponent superstructures of nanomeric size, both in the case of the natural systems and the synthetic mimics.[3] However, detailed insight into the translation of the properties that are encoded in the building blocks to form assemblies of a particular shape or size is still predominantly lacking. The construction of structures in the solid state using self-assembly can be seen as an extension of the formation of aggregates in solution. Although the process of gaining control over structures in the solid state is very complex,[4,5] significant help can be gathered from the understanding of the crystal packing of organic molecules. The design and construction of well-defined and predictable solid-state structures has become a new research area in its own right. It can be foreseen that crystal engineering,[6–9] as the research area has become known, can have numerous applications in the development of electronic devices.[10] It has already been shown that by using self-assembly techniques large organic assemblies can be constructed,[11–13] with hydrogen bonding often being the predominant tool applied. Numerous hydrogen bonded networks and discrete nanoscopic aggregates have been obtained by the self-assembly of building blocks with complementary hydrogen bond donor and acceptor functions.[14–16] A somewhat different strategy is to use molecules which can act as both a hydrogen bond donor and an acceptor, and in this way molecular networks with zeolitic properties,[17] stacked columns,[18–20] interpenetrating molecular ladders,[21] molecular capsules[22–24] and a variety of designed organic structures in the solid state have been assembled.[25] In relatively few cases, however, well-defined self-assembled materials have been constructed based on less directional π−π and electrostatic interactions.[26–28] The 'Molecular Meccano' work of Stoddart, the construction of catenanes and rotaxanes based on donor–acceptor complexation, is an excellent example of this strategy.[29–30]

In our group we have been investigating clip-shaped receptor molecules of type **1** (Chart 1) which are capable of selectively binding dihydroxybenzenes.[31] Binding of these guests is based on hydrogen bonding, π−π interactions, and a 'cavity effect'.[32,33] It is only recently that a further aspect of these receptor molecules has revealed itself: in solution[34–38] as well as in the solid state[39–41] they can form head-to-head dimeric structures, in which the cavity of one molecule is filled by one of the side-walls of its dimeric partner and vice-versa. In this paper we will discuss in detail factors that determine this self-association process in solution and in the crystalline state.

Keywords: crystal engineering; π−π interactions; receptors; molecular modelling.

* Corresponding authors. Tel.: +31-24-3652323; fax: +31-24-3652929; e-mail: jelemans@sci.kun.nl; rowan@sci.kun.nl.

† Present address: Faculty of Chemistry, Institute for Molecular Chemistry, Homogeneous Catalysis, University of Amsterdam, Nieuwe Achtergracht 166, 1018 WV, Amsterdam, The Netherlands.

0040–4020/03/$ - see front matter
PII: S0040-4020(02)01480-1

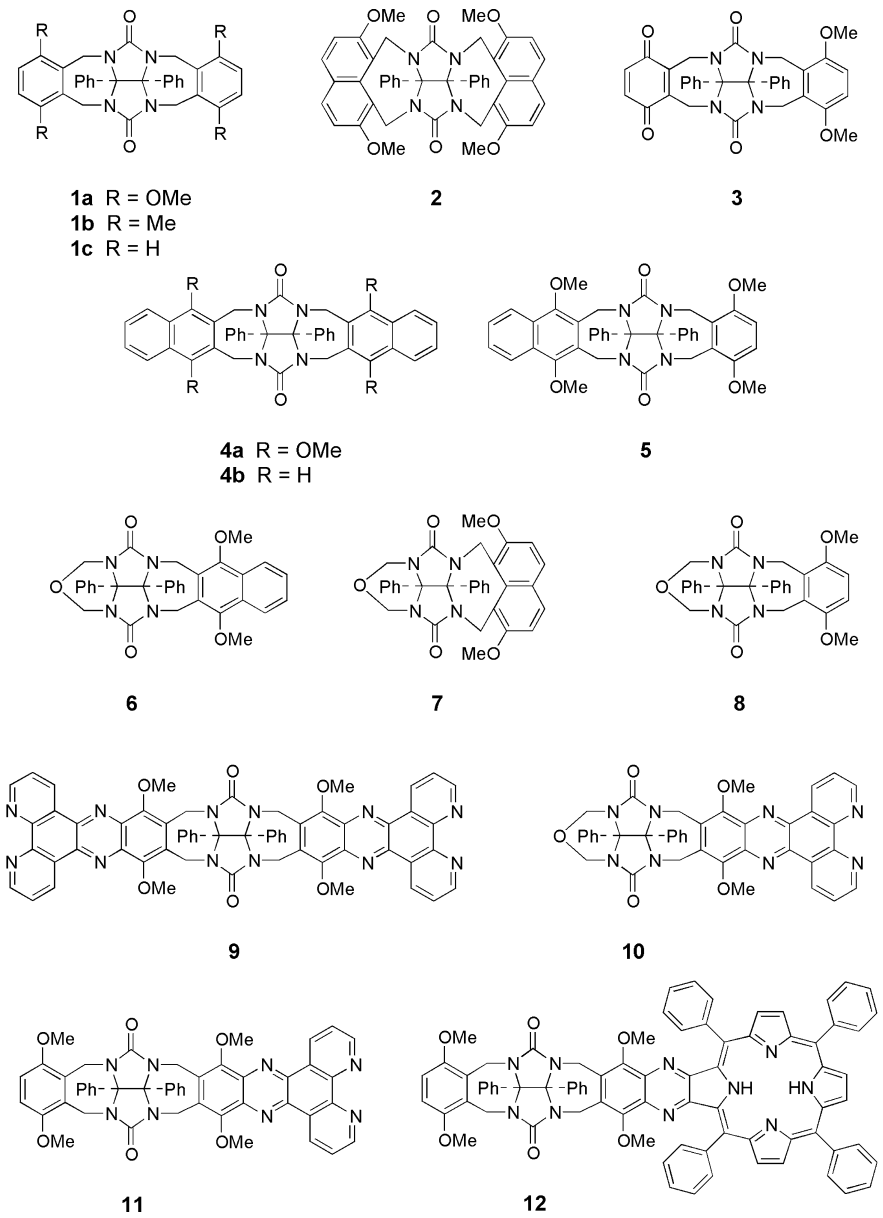

Chart 1.

2. Results and discussion

2.1. Self-association in solution

Careful study of the ^{1}H NMR spectra of molecular clip **1a** (Chart 1) in $CDCl_3$ revealed that upon dilution or an increase in temperature, the resonances of the aromatic side-wall and methoxy protons exhibited considerable downfield shifts. Since for this molecule no conformational changes were expected, a self-association process was proposed involving dimerization of the receptor cavities. To study this in more detail, an NMR dilution titration was carried out in which a plot of the chemical shifts of the proton signals versus concentration could be fitted to a standard equation for a dimerization equilibrium.[42] A dimerization constant $K_{dimer}=16\ M^{-1}$ was calculated for this process. The curve fit also afforded the complexation induced shift (CIS) values, which can give information about the geometry of the self-associated complex, as in the case of host–guest complexes of **1a** with dihydroxybenzenes.[33] A computer program based on the Johnson and Bovey tables was used to calculate the approximate geometries of the dimeric complexes.[43] According to this method compound **1a** dimerized symmetrically, with a side-wall of one clip molecule filling the cavity of the other and vice-versa (Fig. 1). The basis underlying the self-association was thought to be due to two factors: (i) attractive $\pi-\pi$ interactions between the two sets of 1,4-dimethoxybenzene (1,4-DMB) side-walls and (ii) a cavity effect. The latter can be considered to consist of an entropy effect and a solvation effect. The initial $\pi-\pi$ interactions between two side-walls reduce the rotational freedom of the clip molecules, which is an entropically unfavourable process, while the $\pi-\pi$ interactions between the third and fourth side-wall are free of this loss in entropy. The addition of CD_3OD or acetone-d_6 to a concentrated sample of clip **1a** in $CDCl_3$ caused a large downfield shift of the signals of the side-wall protons. This suggests that methanol or acetone molecules break up the

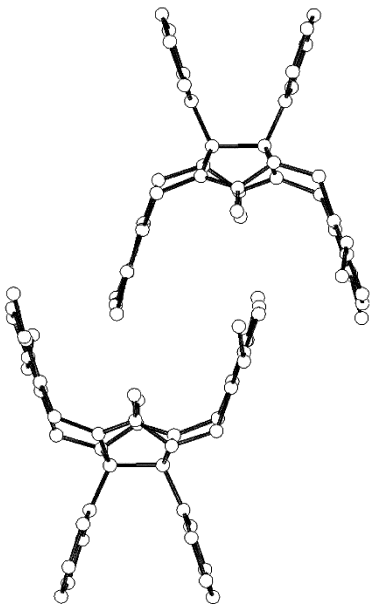

Figure 1. Dimeric structure of clip molecule **1a**, calculated from the CIS values of the NMR dilution titration and the Johnson and Bovey Tables.

dimer, probably because they solvate the cavity of the clip better than chloroform molecules, and/or because of the increase in the dielectric constant, which reduces the π−π interactions between the cavity side-walls.

To obtain better insight into the factors determining the dimerization process, the self-association behaviour of a series of different clip molecules was studied in detail (Table 1). From these studies several trends could be derived. Substitution of the methoxy groups for methyl groups (**1b**) reduced the K_{dimer}, whereas benzene-walled **1c** did not dimerize at all. In the case of these clips the cavity effect and the π−π interactions (which are reduced due to a smaller Van der Waals component) are decreased to such an extent that by dimerization no gain in free energy is obtained.

Table 1. Dimerization constants (K_{dimer}) of molecular clips in $CDCl_3$

Molecular clip	K_{dimer} (M^{-1})
1a	16
1b	<1[a]
1c	7
2	60[b]
3	<5[c]
4a	<1[a]
4b	<1[a]
5	<5[c]
6	<1[a]
7	10[d]
8	<1[a]
9	95
10	<1[a]
11	35
12	<5[c]

Determined by NMR dilution titrations, estimated error 15%.
[a] Chemical shifts were too small to determine a reliable value.
[b] Dimerization constant of the *anti*–*anti*-conformer.
[c] No chemical shifts were observed.
[d] Dimerization constant of the *anti*-conformer.

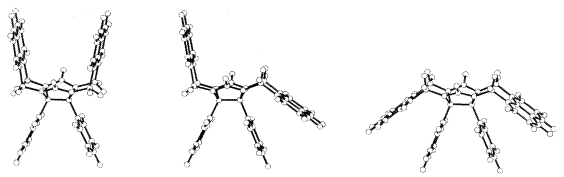

Figure 2. The three conformations of clip **2** which interconvert slowly on the NMR timescale.

Enlarging the side-walls to 1,8-attached 2,7-dimethoxynaphthalene rings (2,7-DMN) (**2** and **7**) gave clip molecules which can adopt different conformations that interconvert slowly on the NMR time scale. These conformations differ by the orientation of the side-wall, which can be *syn* (*s*) or *anti* (*a*) with respect to the phenyl group of the diphenylglycoluril (DPG) part of the molecule (Fig. 2). The observed K_{dimer} for the *aa*-conformer of **2** was significantly larger than that for **1a**. This increase is proposed to be primarily due to a larger contribution of both the π−π interaction and the cavity effect.[‡]

Somewhat surprisingly, clip molecules with 2,3-connected naphthalene side-walls (**4a**,**b**) did not show any self-association behaviour in solution, despite the fact that the cavity effect in these molecules is larger than in clip **1a**. According to calculations using the Hunter and Sanders model,[44] however, the electrostatic contribution to the π−π interaction in dimers of these clips is very repulsive and prohibits complexation of another clip molecule **4**.[§]

Molecules **6** and **8**, which have only one side-wall, also did not show any self-association. Apparently, only one π−π interaction and the absence of a cavity effect does not allow dimeric species in solution to be formed. In the case of **7**, however, the π−π interaction between two 2,7-DMN rings apparently is just large enough to induce some dimerization.

Clip molecules **3** and **5** have one 1,4-DMB and a second, different aromatic side-wall, implying that three dimeric structures are possible. However, the shifts of the proton signals in the dilution titrations were so small that no reliable K_{dimer}-values could be calculated. Apparently, the combination of a cavity effect and only one favourable 1,4-DMB π−π interaction is still not enough to result in a significant dimerization in solution. In the case of a dimer of **3**, the interaction between the *p*-benzoquinone (BQ) side-wall and the 1,4-DMB side-wall was calculated to be unfavourable (see below), which explains the lower self-association.

Functionalization of both side-walls of **1a** with dipyrido[3,2-*a*:2′3′-*c*]phenazine[45] (DPP) groups (clip **9**)

[‡] It was expected that dimers between two *aa* conformers of **2** would be more easily formed than between one molecule in the *aa* conformation and one in an other conformation of **2**, since in the former case two cavity effects and three 'side-wall–side-wall' interactions are involved. Theoretically, the *as* and *ss* conformer could also participate in the dimerization process, however, in the concentration range studied no shifts in the proton signals were observed for these conformers.
[§] Similarly, clips **4a** and **4b** were found to be very poor binders of 1,3-dihydroxybenzene guests, see Ref. 33.

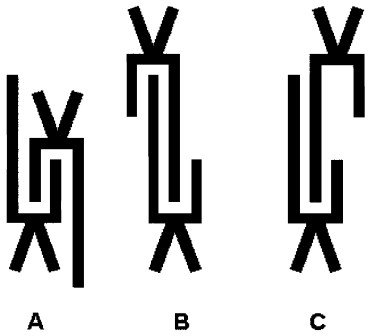

Figure 3. Schematic representation of the three possible dimeric structures of clip **11**.

resulted in an increase in K_{dimer}. The fact that molecule **10** does not display dimerization suggests that the π–π interactions between the side-walls in **9** are not large, and that the driving force behind the dimerization of **9** is mainly an entropy effect due to its large cavity. Clip **11**, however, displayed a higher K_{dimer} compared to **1**, **3** and **5**. This molecule can form dimeric species with different geometries (Fig. 3), i.e. with the two 1,4-DMB rings overlapping (A), with the two DPP rings overlapping (B) or with the DPP surface overlapping with a 1,4-DMB ring (C).[¶] The latter structure, however, is not likely since it is not compact and only one cavity would be occupied.

The dimerization properties of clip molecules **1a**, **9** and **11** were further investigated by temperature-dependent ^{1}H NMR experiments. The spectra were recorded at a constant concentration and the temperature was varied over a wide range. Upon going down in temperature, the signals of the side-wall protons of **1a** shifted strongly upfield, suggesting that more dimeric complex is formed. At 230 K, the signal broadened, which indicated that the equilibrium was becoming slow on the NMR time scale. The fact that the temperature at which this broadening occurred was concentration-dependent confirmed that the observed effects were the result of a dimerization process and not of conformational changes in the molecule. Clip **11** displayed almost the same temperature-dependent behaviour as **1a**. All the signals of the side-walls moved upfield at lower temperatures, except the methoxy signal of the DPP-functionalized side-wall. When, however, the concentration of the sample was increased, the latter signal moved downfield, in contrast to the other signals. This suggests that these methoxy groups have to rotate out of the cavity in order for a dimeric species to be formed. Broadening of all the side-wall protons was observed at 220 K, suggesting that exchange between the monomeric and dimeric species became slow on the NMR time scale. In contrast to the above molecules, the signals of the side-walls of clip **9** moved downfield upon decreasing the temperature, suggesting that the dimer complex became weaker.

To confirm that the K_{dimer}-values are indeed changing at different temperatures, and not the geometry of the dimer structures, the K_{dimer}-values of **9** and **11** were determined at various temperatures, which allowed the calculation of the thermodynamic parameters of the dimerization processes (Table 2). The dimerization of **9** turned out to be entropy driven, whereas for **11** it is enthalpy driven. This suggests that the driving force for the dimerization of **9** is different from that of **11**. In the case of **9**, four large and rigid DPP surfaces are involved in the dimerization process, and therefore the amount of vibrational and rotational entropy, which is lost, is relatively small. In addition, a considerable entropy gain can be expected upon desolvation of these four large surfaces. This is in line with the dimerization of kite-type molecules found by Cram et al., which also appeared to be entropy driven.[46,47] The enthalpically driven dimerization of **11**, apparently, is based on Van der Waals interactions between the two monomeric species of the complex. At 298 K the CIS values of the 1,4-DMB side-wall protons of **11** were different from the CIS values of the corresponding protons of **1a**. The CIS values of the DPP side-wall protons of this compound also differed from those of the side-wall protons of **9**. As a consequence it was difficult to obtain information about the actual dimeric structure of **11** in solution. The CIS values of **9** and **11**, however, were approximately constant over the temperature range studied, which implies that the geometries of the dimeric complexes formed are not temperature-dependent. Since the temperature-dependent behaviour of **1a** and **11** are similar, we tentatively propose that for a dimer of **11** structure A (Fig. 3) is the most likely one.

2.2. Self-association and self-assembly in the solid state

During the solution studies described above the question was raised whether the dimerization interactions between clip molecules in solution would be sufficiently large and geometrically selective to dominate the molecular packing in the solid state. An additional and rather unpredictable factor, however, is that in crystallization processes many packing forces are involved, which are different from solvophobic interactions. In general, one of the driving forces in the case of crystal packing is the necessity to obtain a minimum volume and a maximum density. In the following, the solid-state structures of the clip molecules will be compared with those observed in solution. We succeeded in obtaining X-ray crystal structures of clip molecules **1a**, **2**, **3**, **4a**, **4b**, **5**, **7**, **8** and **12**. To obtain insight

Table 2. Dimerization constants (K_{dimer}) of molecular clips **9** and **11** in $CDCl_3$ at different temperatures, and the calculated thermodynamic parameters

T (K)	**9**		**11**	
	K_{dimer} (M^{-1})	CIS (ppm)	K_{dimer} (M^{-1})	CIS (ppm)
253	50	1.39[a]/0.84[b]	105	1.03[a]/0.74[b]/0.37[c]
273	90	1.30[a]/–[d]	72	1.01[a]/0.69[b]/0.37[c]
298	95	1.48[a]/0.90[b]	35	1.02[a]/–[d]/0.38[c]
318	100	1.31[a]/0.86[b]	28	0.92[a]/0.57[b]/0.39[c]
ΔH (kJ mol^{-1})	7		−14	
ΔS (J mol^{-1} K^{-1})	60		−17	

Determined by NMR dilution titrations, estimated error 15%.
[a] CIS value for the protons of the phenanthroline-ring *ortho* to the N-atom.
[b] CIS value for the protons of the phenanthroline-ring *meta* to the N-atom.
[c] CIS values of the aromatic protons of the 1,4-DMB side-wall.
[d] Signal could not be followed.

[¶] A geometry in which the π–π interactions occur at the outside of the clip can be excluded on the fact that clip **10** does not exhibit any dimerization.

into the packing geometries observed in the crystals, interactions between the aromatic rings of the clips were calculated using the Hunter and Sanders model.[44] To get an idea of the interaction energies as a function of the geometry, energy profiles were calculated for the π−π interactions between several different aromatic moieties, viz. the combinations 1,4-DMB-1,4-DMB, 1,4-DMB-BQ, 1,4-DMN-1,4-DMN, 2,7-DMN-2,7-DMN, and naphthalene-naphthalene.

From the dimerization studies in solution, it can be concluded that the interaction between two 1,4-DMB rings is very favourable. In Figure 4, the interactions are shown between two 1,4-DMB rings which are positioned cofacially at a distance of 3.4 Å. The energy surface was calculated for two rings with their methoxy groups pointing in the same direction, resulting in a symmetric profile, and for rings with their methoxy groups pointing in opposite directions. Each surface shows three large energy maxima, which are the result of the direct overlap of the methoxy groups, resulting in a Van der Waals repulsion. A direct overlap is also disfavoured due to repulsive electrostatic interactions between the aromatic rings. In the symmetrical case (Fig. 4a), it is evident that an offset geometry is more favourable than a direct overlap. In the unsymmetrical case (Fig. 4b), two large energy minima (x=−3 Å, y=−2 Å and x=3 Å, y=-2 Å) are observed, both at an offset geometry (in addition, a smaller minimum is observed at (x=0 Å, y=3 Å)). It can therefore be concluded that the proposed offset geometry of the 1,4-DMB rings in the dimeric structure of **1a** in solution (Fig. 1) is very similar to the one of the calculated minima in Figure 4b.

The offset for the minima in Figure 4b is approximately (x=3 Å, y=-2 Å). These minima are dependent on the distance between the aromatic rings (Fig. 4c). The optimum x-offset distance is shifted by approximately 1.6 Å if the aromatic rings are pulled 0.3 Å further apart. The energy minimum is relatively constant when the rings are between 3.4 and 3.8 Å apart. Once fixed at a certain distance, it is of interest to know how the energy changes when the geometry of the rings is varied. As can been seen in Figure 4c, the energy minima are relatively global: within the range of 2 kJ mol^{-1} the aromatic ring can move approximately 1.5 Å in both directions.

The solution and X-ray structures of the five clip molecules having 1,4-DMB side-walls, in spite of additional interactions involved in crystal packing, showed great similarity with the calculated minimum geometries in Figure 4b (Table 3). For clips **3** (Fig. 5a) and **12**[35] (Fig. 5b) the observed crystal geometry is identical to the dimeric geometry derived from the ^{1}H NMR studies in solution. The molecules are arranged in well-defined dimers, in which interactions are present between the 1,4-DMB rings. The geometry in both cases is an offset one, similar to the geometry predicted by the calculations. The distances between the planes of the 1,4-DMB rings is approximately 3.4 Å. Somewhat surprising in the case of **3** is that the interaction between two 1,4-DMB rings is more favourable than between an electron poor BQ and an electron rich

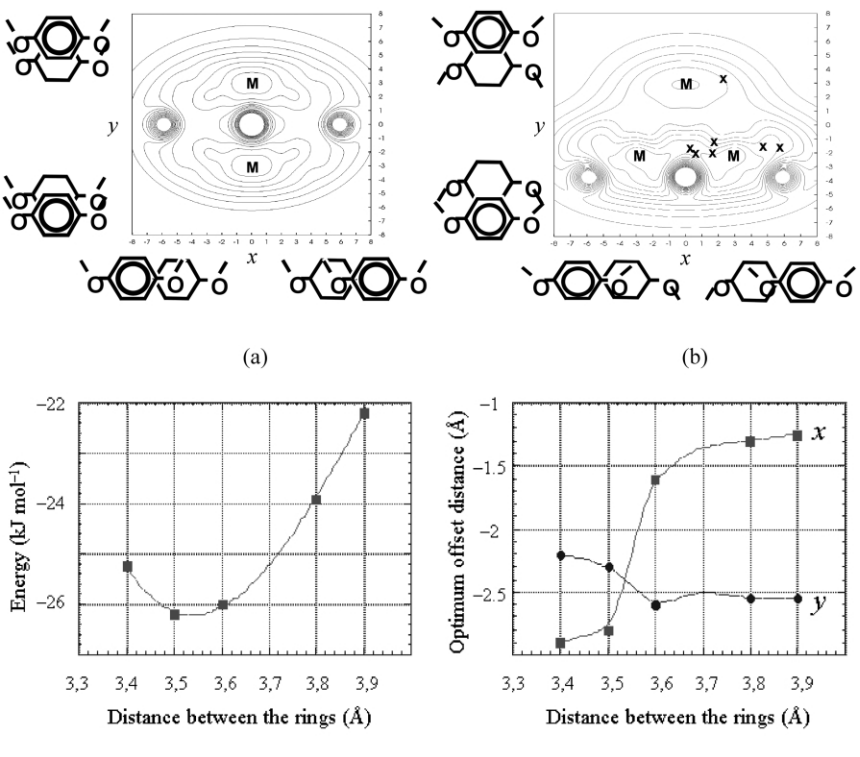

Figure 4. (a,b) Calculated energy surfaces for two interacting 1,4-DMB rings as a function of x- and y-offset. (a) Symmetric overlap of rings. (b) Non-symmetric overlap of rings. **M**=calculated minima, contours at 2.5 kJ mol^{-1}, ×-marks correspond to the x- and y-offsets between interacting 1,4-DMB rings observed in the various X-ray structures (see also Table 3). (c) The energy minimum (left) and the position (x and y offset) of the energy minimum (right) as a function of the distance between the two 1,4-DMB rings. The curves correspond to the right minimum in (b).

Table 3. Summary of the interactions between the aromatic side-walls in the X-ray structures of clip molecules

Molecular clip	Type of interaction[a]	*z*-Offset (Å)	*x*-Offset (Å)	*y*-Offset (Å)	Calculated energy (kJ mol^{-1})[b]
1a	B	4.23	4.66	−1.72	−16
	B	3.73	2.16	+3.14	−16
2	N	3.45	1.56	+3.46	
3	B	3.43	0.60	−2.05	−22
4a	N	3.60	1.43	−2.73	
4b	N	3.53	1.09	−2.45	
	N	3.57	1.02	−2.96	
5	B	2.99	5.71	−1.81	−17
	N	3.64	1.80	−2.45	
7	N	3.43	0.51	+3.46	
8	B	4.20	1.64	−2.06	−21
	B	3.97	1.68	−1.32	−20
12	B	3.31	0.15	−1.89	−21

[a] B=between two benzene surfaces, N=between two naphthalene surfaces.
[b] According to the Hunter and Sanders model.

1,4-DMB ring. This is contrary to what is expected on the basis of the donor–acceptor theory.[48–50] Calculations which were performed using the Hunter and Sanders model (a similar energy surface was calculated as between two 1,4-DMB rings) predicted that the interaction between a BQ ring and a 1,4-DMB ring indeed is less favourable by 4 kJ mol^{-1} at the geometry found in the X-ray structure. If the interactions are examined more closely it can be seen that the electrostatic interaction between a BQ and a 1,4-DMB ring is actually 1 kJ mol^{-1} more favourable than the interaction between two 1,4-DMB rings, as would be expected. This increase in the electrostatic interaction, however, is not large enough to overcome the drop in Van der Waals interaction energy, which is 5 kJ mol^{-1} less favourable in the case of BQ–1,4-DMB interaction. Consequently, the overall interaction between two 1,4-DMB moieties is more favourable.

Mono-walled clip **8** also showed a solid-state packing with noticeable 1,4-DMB interactions. Dimeric structures are present, which also have favourable interactions with neighbouring dimers (Fig. 5c). These offset interactions are calculated to be favourable, although the distance between the aromatic surfaces is relatively large (3.9 Å for

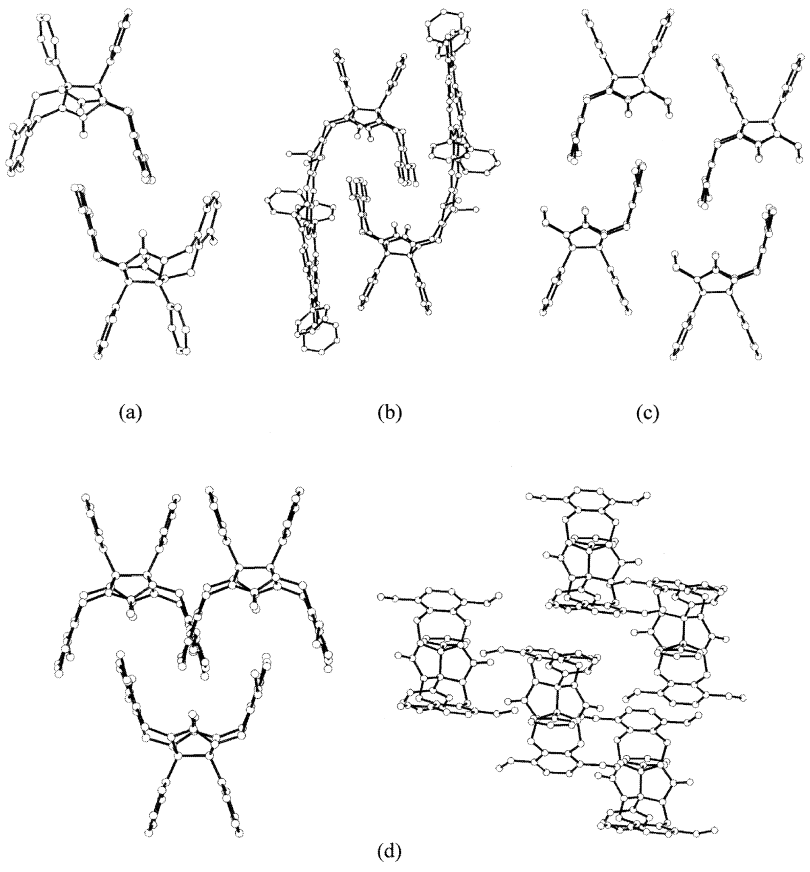

Figure 5. (a) X-Ray structure of clip molecule **3**. (b) X-Ray structure of clip molecule **12**. (c) X-Ray structure of clip molecule **8**. (d) X-Ray structure of clip molecule **1a**, side view (left) and top view (right).

the interaction at the inside of the clip and 4.2 Å at the outside). It can be seen in Figure 4c, however, that even at a distance of 3.9 Å there is still a significant π−π interaction.

In the X-ray structure of **1a**,[32] the clips are not arranged in discrete dimers, but in polymeric arrays (Fig. 5d), in which each clip has an offset interaction with two adjacent clip molecules. The next array of clip molecules is inverted with respect to the first array. Each molecule in the array has an interaction with four molecules from the rows on either side. These four interactions apparently are more favourable than an arrangement in discrete dimers. According to our calculations, however, the 1,4-DMB interactions do not have a specific minimum energy, but rather a general region in which the energy is low (see above).

As expected, the large 1,4-DMN π-surfaces dominated the geometry of the crystal structure of **5** (Fig. 6b). The distance between two 1,4-DMN rings of adjacent molecules is 3.64 Å. According to calculations the observed offset geometry between these rings (x=1.80 Å, y=−2.45 Å) is favourable. The geometry for the optimal interaction between the 1,4-DMN rings cannot be achieved if the molecules form a dimeric structure, in which the cleft of one molecule is filled with the side-wall of another molecule. A relatively small interaction between two 1,4-DMB rings having a large offset (x=5.71 Å, y=−1.81 Å) is also observed in the X-ray structure (Fig. 6a).

The above described geometric packing of the 1,4-DMN moieties is also found in the solid state structure of clip **4a** (Fig. 6c).[51] The outside distance between two aromatic surfaces is 3.60 Å, with an offset of (x=1.43 Å, y=−2.73 Å), which is just offset from the calculated minimum (Fig. 7b). In the case of this clip all the methoxy groups point into the cavity. The molecules of **4a** contain a large cavity, which is filled by the phenyl group of the DPG unit of a neighbouring molecule (Fig. 6d). This molecule is twisted, with the phenyl groups having face-to-edge interactions with each of the naphthalene side-walls of the underlying clip molecule.

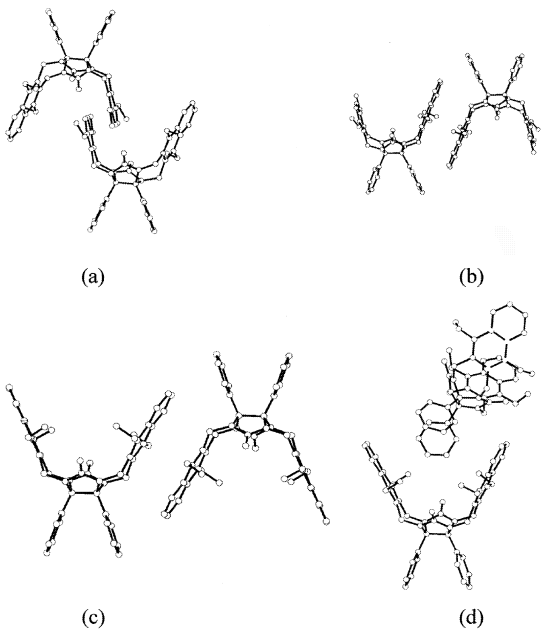

Figure 6. (a,b) The two types of interactions observed in the X-ray structure of clip molecule **5**. (c,d) The two types of interactions observed in the X-ray structure of clip molecule **4a**.

One may ask the question how important the methoxy groups are in the interactions between the 1,4-DMN aromatic rings. According to our calculations, the Van der Waals energy is optimal when the aromatic rings are totally overlapping. In the case of 1,4-DMN surfaces, however, a Van der Waals repulsion is observed as a result of the protons of the methoxy groups making close contact with each other. Beside this repulsion at direct overlap, the Van der Waals force is attractive and only slightly dependent on the geometry. The electrostatic contribution, which is repulsive at direct overlap, is in contrast to the Van der Waals energy very sensitive to the geometric arrangement and falls off rapidly as the displacement increases. In the case of the electrostatic interaction, the methoxy groups play a significant role, making some of the carbon atoms of the ring more electron rich and others electron poor (Hammett values for the *para* and *meta* position are 0.12 and −0.27, respectively).[52] As a result, the overall energy surface of the interaction between two 1,4-DMN rings is less smooth than the energy surface of the interaction between two naphthalene rings (Fig. 7). This, of course, leads to a different optimal offset geometry, and thus different interactions in the solid state. Two main offset interactions between the side-walls are found in the X-ray structure of clip **4b** (Fig. 8). The first one involves two side-walls that are partly filling the clefts of two opposing clip molecules. The two aromatic rings have a distance of 3.53 Å, and an offset of (x=1.09 Å, y=−2.45 Å). The second interaction is at the outside of the clip molecule and is similar to the interaction observed for **4a**, viz. phenyl rings that partly fill the cavity of another clip molecule. The distance between the rings is 3.57 Å, and the offset is (x=1.02 Å, y=−2.96 Å).[‖]

In solution, clip molecules **2** and **7** both show self-association, due to a favourable interaction between the 2,7-DMN side-walls. Calculations revealed that there are two regions of optimal geometry, differing in energy by 2.5 kJ mol^{-1} (Fig. 9a). In the X-ray structure of clip **7**, the geometry with the lowest calculated energy is observed (Fig. 9b). The interaction takes place at the outside of the clip. The distance between the aromatic surfaces is 3.42 Å, and the offset (x=0.51 Å, y=+3.46 Å). The molecules are packed in dimers, with a small interaction between adjacent dimers. A CH_3−aromatic interaction is observed (distance is approximately 3.04 Å, see Fig. 9a), however, this is not expected to contribute much to the overall interaction energy.[53] Clip molecule **2**, which has two 2,7-DMN side-walls could only be crystallized in the presence of a nitrobenzene guest molecule, which means that the cavity of the clip is already filled and that a dimeric structure cannot be adopted. Based on the calculations it was predicted that the major interaction in the X-ray structure of **2** would be between the side-walls of adjacent clip molecules. Figure 9c

[‖] A chloroform molecule is incorporated in the crystal, forming a weak hydrogen bond with the carbonyl group of the DPG unit (CCl_3H−OC distance is 2.19 Å).

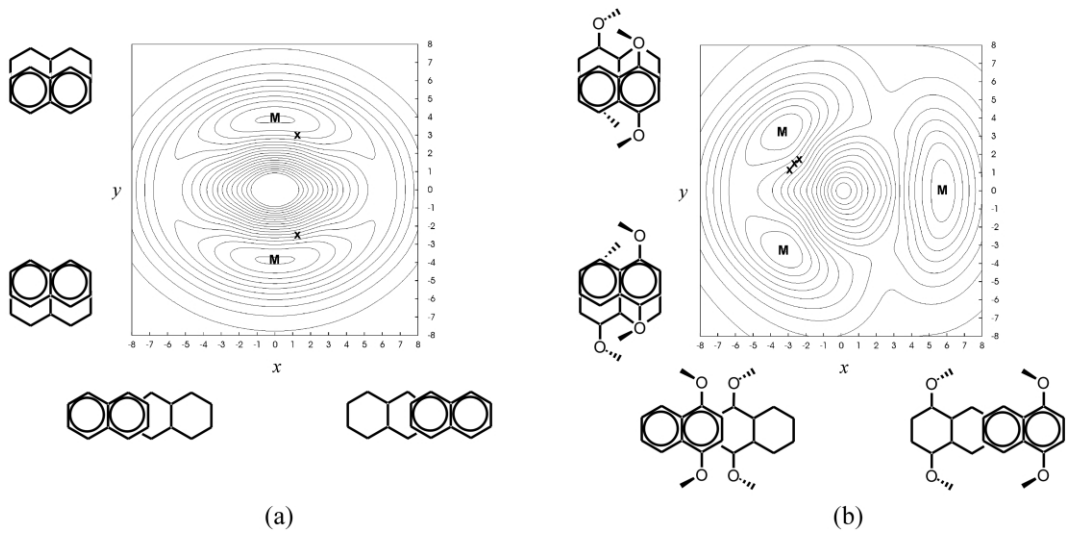

Figure 7. The interaction energies between (a) two naphthalene and (b) two 1,4-DMN surfaces as calculated with the Hunter and Sanders model; **M**=calculated minima, contours at 2.5 kJ mol^{-1}, ×-marks correspond to the *x*- and *y*-offsets between interacting naphthalene or 1,4-DMN rings observed in the various X-ray structures (see also Table 3).

shows that the most favoured interaction is at an inverted and offset geometry. Neighbouring molecules are pointing in opposite direction and stack with their side-walls at exactly the calculated optimum offset distance, which is 3.45 Å. All the stacked rows are independent of each other. In addition, the nitrobenzene guest molecules have an optimal stacking geometry with the 2,7-DMN side-walls.

Finally, it should be noted that in the solid-state structures of the different clip molecules the phenyl groups of the DPG unit are often observed to be within close proximity of an aromatic side-wall, which obviously leads to a favourable interaction. This is particularly the case in the X-ray structure of clip **12**, which has a large porphyrin unit nearby these phenyl groups (Fig. 5b). In all examples the distances between the above mentioned phenyl groups and the aromatic side-walls were between 3.5 and 3.6 Å. These are obviously important interactions in the solid state structure, but they are not expected to dominate the geometry of the structures in solution.

3. Conclusions

In Table 3 the important distances and offsets between aromatic rings found in the solid-state structures of clip molecules are summarized. Comparison of the X-ray geometries with the optimal geometries calculated using the Hunter and Sanders model shows that there is reasonable agreement between the calculations and the experimental results. Although the Hunter and Sanders model is relatively simple, it is useful in calculating the optimum geometries and relative interaction energies between aromatic molecules. Using this computational tool, we have been able to interpret structures in solution and in the solid state. In solution the poor solvation of the cavity by solvent molecules and favourable $\pi-\pi$ stacking interactions play an important role in the dimer formation of the clip molecules. In the solid state these $\pi-\pi$ interactions together with crystal packing forces determine the structures. The $\pi-\pi$ interactions direct the packing arrangement, but they are not as geometrically stringent as hydrogen bonds. In the systems described here, an approximate region of favourable interaction between aromatic rings was observed. The optimum calculated interaction geometry, therefore, is not always exactly the one found in the X-ray structure. A crystal packing that results in four weaker intermolecular interactions, for example, can be more favourable than one stronger interaction, as was seen for clip **1a**. Even more remarkable, it has been demonstrated that an interaction between two electron rich surfaces can be more favourable in the X-ray structure than an expected strong interaction between an electron poor and an electron rich surface (clip **3**).

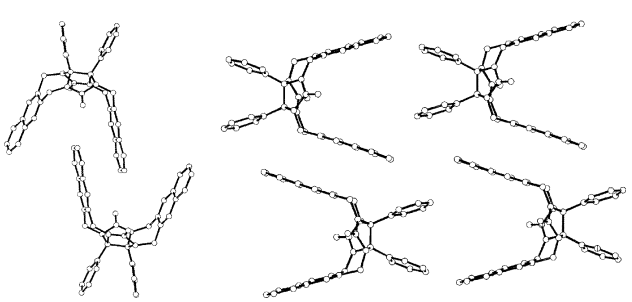

Figure 8. The two types of interactions observed in the X-ray structure of clip molecule **4b**.

Using the knowledge obtained from interactions in solution and in the solid state, we may be able in the near future to predict with a higher precision the most dominant aromatic interaction and hence the probable crystal packing arrangements. Although the present study is only a very first step towards the use of clip molecules in the rational design of organic solid state lattices and nanosized superstructures, we feel that we already have a reasonable understanding of the packing forces involved in the crystallization of this type of molecules. Future work will be focused on the construction of well-defined solid state materials using the self-assembling properties of these molecular clips, with geometries which can be precisely controlled by

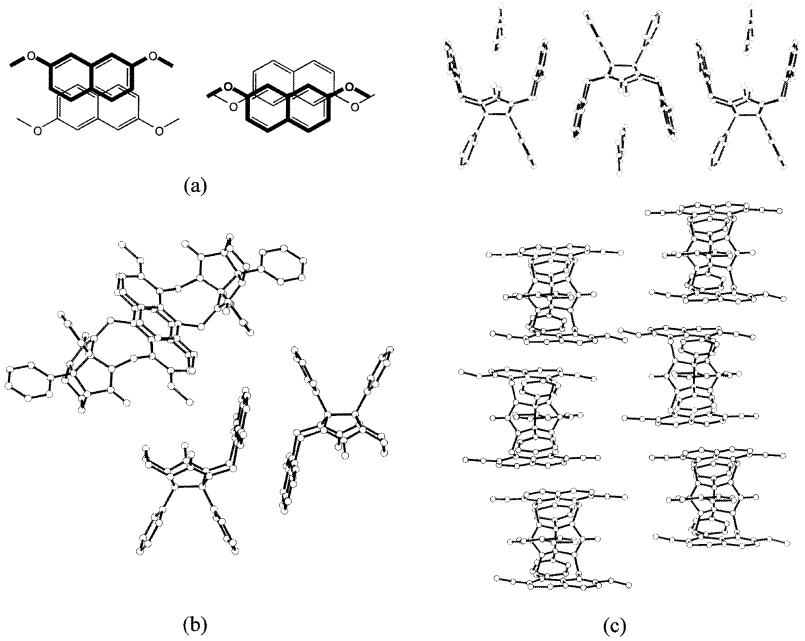

Figure 9. (a) The two optimum interactions between two 2,7-DMN rings according to calculations using the Hunter and Sanders model. The geometry on the right is 2.5 kJ mol^{-1} more favourable than the one on the left. (b) The two types of interactions in the X-ray structure of clip molecule **7**. (c) The X-ray structure of the complex of clip molecule **2** and nitrobenzene, side-view (top) and top view (bottom).

the nature of the cavity side-walls and their substitution pattern.

4. Experimental

4.1. General

The syntheses of the molecules discussed in this paper have been previously described.[54] Dimerization constants were determined by diluting the samples from their maximum solubility (varying from 10 to 40 mM) to their minimum concentrations required for detection of signals by ^{1}H NMR (approximately 0.1 mM). In general the chemical shifts of the side-wall protons were followed as function of the concentration of the clips. The obtained curves were fitted using the following equation:

$$\delta_{obs} = \delta_m + \frac{(\delta_m + \delta_d)(1 + 4cK_{dimer} - \sqrt{(1 + 8cK_{dimer})})}{4cK_{dimer}}$$

in which c is the concentration of the molecule (in M), δ_{obs} is the observed chemical shift, δ_m the chemical shift of the monomer and δ_d the chemical shift of the dimer (all shifts in Hz). The ^{1}H NMR measurements were carried out on Bruker AM 400 MHz and WM 200 MHz instruments.

4.2. X-Ray structures

The X-ray structures of **1a** and **4a** (CSD-refcode 'JISDEU') were taken from Refs. 32,51, respectively. Detailed crystallographic data of compounds **4b**[55] (CSD-refcode 'TIXSUO') and **5**[56] (CSD-refcode 'ROBWEK') are described in the literature. Crystallographic data (excluding structure factors) for the structures of compounds **2** (CCDC 189569), **3** (CCDC 195075), **7** (CCDC 195074), **8** (CCDC 195073) and **12** (CCDC 189568) have been deposited with the Cambridge Crystallographic Data Centre. Copies of the data can be obtained, free of charge, on application to CCDC, 12 Union Road, Cambridge, CB2 1EZ, UK [fax: +44(0)-1223-336033 or e-mail: deposit@ccdc.ca.ac.uk].

4.2.1. Crystal data for the complex of 2 and nitrobenzene. $C_{51}H_{44}Cl_3N_5O_8$, M_r=941.26, T=293(2) K, triclinic, space group P-1, a=12.188(9) Å, b=12.161(12) Å, c=17.756(13) Å, α=103.33(13)°, β=104.74°, γ=107.70°, V=2285(3) Å^3, Z=2, ρ_{calcd}=1.397 g cm^{-3}, Mo Kα radiation, μ=0.78 cm^{-1}.

4.2.2. Crystal data for 3. $C_{35}H_{29}N_4O_6Cl_3$, M_r=708.0, T=293 K, monoclinic, space group $P2_1/c$, a=13.0326(6) Å, b=18.858(2) Å, c=13.5561(11) Å, β=100.800(7)°, V=3273 Å^3, Z=4, ρ_{calcd}=1.437 g cm^{-3}, Mo Kα radiation, μ=3.30 cm^{-1}.

4.2.3. Crystal data for 4b. $C_{40}H_{30}N_4O_2{\cdot}CHCl_3$, M_r=718.05, T=208 K, triclinic, space group P-1, a=9.302(2) Å, b=12.981(2) Å, c=15.765(2) Å, α=65.91(2)°, β=76.40(2)°, γ=80.15(1)°, V=1682.9 Å^3, Z=2, ρ_{calcd}=1.417 g cm^{-3}, Mo Kα radiation, μ=3.17 cm^{-1}.

4.2.4. Crystal data for 5. $C_{42}H_{38}N_4O_6Cl_6$, M_r=907.5, T=208 K, monoclinic, space group $P2_1/n$, a=12.5667(9) Å, b=19.1713(12) Å, c=17.4311(11) Å, β=91.676(6)°, V=4198 Å^3, Z=4, ρ_{calcd}=1.436 g cm^{-3}, Mo Kα radiation, μ=4.61 cm^{-1}.

4.2.5. Crystal data for 7. $C_{32}H_{28}N_4O_5$, M_r=548.6, T=208 K, orthorombic, space group $Pbca$, a=12.3332(16) Å, b=27.874(2) Å, c=15.1246(15) Å, V=5199 Å^3, Z=8, ρ_{calcd}=1.402 g cm^{-3}, Mo Kα radiation, μ=0.90 cm^{-1}.

4.2.6. Crystal data for 8. $C_{28}H_{26}N_4O_5$, M_r=498.5, T=293 K, triclinic, space group P-1, a=8.2849(15) Å, b=12.525(2) Å, c=13.438(4) Å, α=116.83(2)°, β=105.17(3)°, γ=90.07(2)°, V=1189 Å^3, Z=2, ρ_{calcd}=1.392 g cm^{-3}, Mo Kα radiation, μ=0.91 cm^{-1}.

4.2.7. Crystal data for 12. $C_{84}H_{70}N_{10}O_7$, M_r=1331.50, T=173.(2) K, monoclinic, space group $P2_1/n$, a=14.8272(12) Å, b=24.0148(25) Å, c=19.1212(13) Å, β=99.048(69)°, V=6723.8(10) Å^3, Z=4, ρ_{calcd}=1.315 g cm^{-3}, Mo Kα radiation, μ=0.791 cm^{-1}.

4.3. Computational methods

Calculations were performed on Silicon Graphics Challenge and Silicon Graphics Indigo II workstations. The molecular structures were generated with the Sybyl program, and optimised by calculations using the MOPAC program and the ESP option for the charges. The charges and coordinates were taken from the output file of this program. The keyword PI in MOPAC splits the final density matrix into π and σ contributions. The π densities at the diagonal of the density matrix were used as the π charges above and below the plane of the aromatic molecule in the case of the calculations using the Hunter and Sanders model. Energy surfaces were calculated, using an electrostatic and a Van der Waals potential, by changing the x and y coordinates of one of the two surfaces in a stepwise manner.

References

1. Mann, S. *Nature* **1993**, *365*, 499–505.
2. Whitesides, G. M.; Mathias, J. P.; Seto, C. T. *Science* **1991**, *254*, 1312–1319.
3. Ringsdorf, H.; Schlarb, B.; Venzmer, J. *Angew. Chem.* **1988**, *100*, 117–162.
4. Perlstein, J. *J. Am. Chem. Soc.* **1992**, *114*, 1955–1963.
5. Dunitz, J. D.; Gavezzotti, A. *Acc. Chem. Res.* **1999**, *32*, 677–684.
6. Desiraju, G. R. *Crystal Engineering: The Design of Organic Solids*. Elsevier: Amsterdam, 1989.
7. Russell, V. A.; Ward, M. D. *Chem. Mater.* **1996**, *8*, 1654–1666.
8. Desiraju, G. R. *Chem. Commun.* **1997**, 1475–1482.
9. Ashton, P. R.; Fyfe, M. C. T.; Hickingbottom, S. K.; Menzer, S.; Stoddart, J. F.; White, A. J. P.; Williams, D. J. *Chem. Eur. J.* **1998**, *4*, 577–589.
10. Service, R. F. *Science* **1994**, *265*, 316–318.
11. Bernstein, J.; Davis, R. E.; Shimoni, L.; Chang, N.-L. *Angew. Chem. Int. Ed. Engl.* **1995**, *34*, 1555–1573.
12. Lawrence, D. S.; Jiang, T.; Levett, M. *Chem. Rev.* **1995**, *95*, 2229–2260.
13. Balagurusamy, V. S. K.; Ungar, G.; Percec, V.; Johansson, G. *J. Am. Chem. Soc.* **1997**, *119*, 1539–1555.
14. Subramanian, S.; Zaworotko, M. J. *Coord. Chem. Rev.* **1994**, *137*, 357–401.
15. Schwiebert, K. E.; Chin, D. N.; MacDonald, J. C.; Whitesides, G. M. *J. Am. Chem. Soc.* **1996**, *118*, 4018–4029.
16. Chin, D. N.; Palmore, G. T. R.; Whitesides, G. M. *J. Am. Chem. Soc.* **1999**, *121*, 2115–2122.
17. Brunet, P.; Simard, M.; Wuest, J. D. *J. Am. Chem. Soc.* **1997**, *119*, 2737–2738.
18. Endo, K.; Sawaki, T.; Koyanagi, M.; Kobayashi, K.; Masuda, H.; Aoyama, Y. *J. Am. Chem. Soc.* **1995**, *117*, 8341–8352.
19. Aoyama, Y.; Endo, K.; Anzai, T.; Yamaguchi, Y.; Sawaki, T.; Kanehisa, N.; Hashimoto, H.; Kai, Y.; Masuda, H. *J. Am. Chem. Soc.* **1996**, *118*, 5562–5571.
20. Dewa, T.; Endo, K.; Aoyama, Y. *J. Am. Chem. Soc.* **1998**, *120*, 8933–8940.
21. Fujita, M.; Kwon, Y. J.; Sasaki, O.; Yamaguchi, K.; Ogura, K. *J. Am. Chem. Soc.* **1995**, *117*, 7287–7288.
22. Rebek, Jr. J. *Chem. Soc. Rev.* **1996**, 255–264.
23. Conn, M. M.; Rebek, Jr. J. *Chem. Rev.* **1997**, *97*, 1647–1668.
24. Rebek, Jr. J. *Acc. Chem. Res.* **1999**, *32*, 278–286.
25. Lehn, J.-M. *Supramolecular Chemistry*. VCH: Weinheim, 1995.
26. Blake, A. J.; Champness, N. R.; Khlobystov, A. N.; Lemenovskii, D. A.; Li, W.-S.; Schröder, M. *Chem. Commun.* **1997**, 1339–1340.
27. Rovira, C. *Chem. Eur. J.* **2000**, *6*, 1723–1729.
28. Bosch, E.; Radford, R.; Barnes, C. K. *Org. Lett.* **2001**, *3*, 881–883.
29. Amabilino, D. B.; Anelli, P. R.; Ashton, P. R.; Brown, G. R.; Córdova, E.; Godínez, L. A.; Hanes, W.; Kaifer, A. E.; Philp, D.; Slawin, A. M. Z.; Spencer, N.; Stoddart, J. F.; Tolley, M. S.; Williams, D. J. *J. Am. Chem. Soc.* **1995**, *117*, 11142–11170.
30. Cabezon, B.; Cao, J. G.; Raymo, F. M.; Stoddart, J. F.; White, A. J. P.; Williams, D. J. *Chem. Eur. J.* **1997**, *6*, 2262–2273.
31. Rowan, A. E.; Elemans, J. A. A. W.; Nolte, R. J. M. *Acc. Chem. Res.* **1999**, *32*, 995–1006.
32. Sijbesma, R. P.; Kentgens, A. P. M.; Lutz, E. T. G.; van der Maas, J. H.; Nolte, R. J. M. *J. Am. Chem. Soc.* **1993**, *115*, 8999–9005.
33. Reek, J. N. H.; Priem, A. H.; Engelkamp, H.; Rowan, A. E.; Elemans, J. A. A. W.; Nolte, R. J. M. *J. Am. Chem. Soc.* **1997**, *119*, 9956–9964.
34. Reek, J. N. H.; Kros, A.; Nolte, R. J. M. *Chem. Commun.* **1996**, 245–247.
35. Reek, J. N. H.; Rowan, A. E.; de Gelder, R.; Beurskens, P. T.; Crossley, M. J.; de Feyter, S.; de Schryver, F.; Nolte, R. J. M. *Angew. Chem. Int. Ed. Engl.* **1997**, *36*, 361–363.
36. Elemans, J. A. A. W.; de Gelder, R.; Rowan, A. E.; Nolte, R. J. M. *Chem. Commun.* **1998**, 1553–1554.
37. Elemans, J. A. A. W.; Slangen, R. R. J.; Rowan, A. E.; Nolte, R. J. M. *J. Incl. Phenom. Macrocycl. Chem.* **2001**, *41*, 65–68.
38. Elemans, J. A. A. W.; Rowan, A. E.; Nolte, R. J. M. *J. Am. Chem. Soc.* **2002**, *124*, 1532–1540.
39. Holder, S. J.; Elemans, J. A. A. W.; Barberá, J.; Rowan, A. E.; Nolte, R. J. M. *Chem. Commun.* **2000**, 355–356.
40. Holder, S. J.; Elemans, J. A. A. W.; Donners, J. J. J. M.; Boerakker, M. J.; de Gelder, R.; Barberá, J.; Rowan, A. E.; Nolte, R. J. M. *J. Org. Chem.* **2001**, *66*, 391–399.
41. Elemans, J. A. A. W.; Boerakker, M. J.; Holder, S. J.; Rowan, A. E.; Cho, W.-D.; Percec, V.; Nolte, R. J. M. *Proc. Natl Acad. Sci. USA* **2002**, *99*, 5093–5098.
42. Abraham, R. J.; Rowan, A. E.; Mansfield, K. E.; Smith, K. M. *J. Chem. Soc., Perkin Trans. 2* **1991**, 515–521.
43. Johnson, Jr. C. S.; Bovey, F. A. *J. Chem. Phys.* **1958**, *29*, 1012–1014.
44. Hunter, C. A.; Sanders, J. K. M. *J. Am. Chem. Soc.* **1990**, *112*, 5525–5534.

45. Beeson, J. C.; Fitzgerald, L. J.; Gallucci, J. C.; Gerkin, R. E.; Rademacher, J. T.; Czarnik, A. W. *J. Am. Chem. Soc.* **1994**, *116*, 4621–4622.
46. Bryant, J. A.; Knobler, C. B.; Cram, D. J. *J. Am. Chem. Soc.* **1990**, *112*, 1254–1255.
47. Bryant, J. A.; Ericson, J. L.; Cram, D. J. *J. Am. Chem. Soc.* **1990**, *112*, 1255–1256.
48. Briegleb, G. *Electronen-Donator–Acceptor-Komplexe*. Sprongler: Berlin, 1961.
49. Morakuma, K. *Acc. Chem. Res.* **1977**, *10*, 294–300.
50. Hunter, C. A. *Angew. Chem. Int. Ed. Engl.* **1993**, *32*, 1584–1586.
51. Bosman, W. P.; Beurskens, P. T.; Admiraal, G.; Sijbesma, R. P.; Nolte, R. J. M. *Z. Kristallogr.* **1991**, *197*, 305–308.
52. Hansch, C.; Leo, A.; Taft, R. W. *Chem. Rev.* **1991**, *91*, 165–195.
53. Nishio, M.; Hirota, M. *Tetrahedron* **1989**, *45*, 7201–7245.
54. Reek, J. N. H.; Elemans, J. A. A. W.; Nolte, R. J. M. *J. Org. Chem.* **1997**, *62*, 2234–2243.
55. Bosman, W. P.; Smits, J. M. M.; de Gelder, R.; Reek, J. N. H.; Nolte, R. J. M. *J. Chem. Cryst.* **1996**, *26*, 365–368.
56. Bosman, W. P.; Smits, J. M. M.; de Gelder, R.; Reek, J. N. H.; Elemans, J. A. A. W.; Nolte, R. J. M. *J. Chem. Cryst.* **1997**, *27*, 75–79.